Available online at www.sciencedirect.com
ScienceDirect
Mendeleev Commun., 2017, **27**, 634–636
Mendeleev Communications

Facile synthesis of 2D silver nanocrystals by a gas–solution interface technique

Larisa B. Gulina,*[a] Valeri P. Tolstoy[a] and Elena V. Tolstobrov[a,b]

[a] *Institute of Chemistry, St. Petersburg State University, 199034 St. Petersburg, Russian Federation.*
E-mail: l.gulina@spbu.ru
[b] *OOO NPP 'Galus', 191106 St. Petersburg, Russian Federation*

DOI: 10.1016/j.mencom.2017.11.033

The templateless and surfactant-free facile synthesis of 2D silver nanocrystals was carried out for the first time by a gas–solution interface technique using an aqueous solution of AgOAc and gaseous N_2H_4 as reactants.

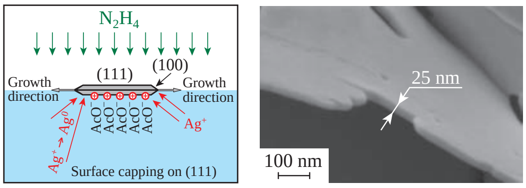

$AgOAc_{(solution)} + N_2H_{4\,(gas)} \longrightarrow$ Ag 2D crystals$_{(solid)}$

Silver nanoparticles are of considerable current interest due to their excellent optical, electrical and chemical properties. The shape-controlled synthesis of silver nanostructures is very important for the design of promising materials, in particular, to be used as ideal building blocks for micro- and nanodevices.[1–4] The silver nanoparticles are also of importance for optics, plasmonics,[5–10] sensors,[11–13] catalysis[14–17] and biomedicine.[18–20] As for 2D silver nanoparticles (nanoplates), they are thermodynamically unstable due to their high surface energy.[21] Consequently, new methods of fabrication of such 2D nanoparticles are very important to improve their properties and to make more affordable their manufacturing technology. Wet chemical synthetic protocols with the use of cetyltrimethylammonium bromide,[22] polyvinylpyrrolidone,[23] Ag seeds with insoluble silver salt[24] or modified polyol route[25,26] have been employed to obtain silver nanoparticles in solution. Crystallization on a polymer surface[27] or redox of copper particles on ITO[28] were applied to the synthesis of immobilized silver nanosheets.

Recently, a facile gas–solution interface technique (GSIT) was successfully used to synthesize well-known inorganic materials with the morphology of thin films and microtubes.[29–34] The interaction between the cations of salt solution and a gaseous reactant plays an important role in this synthesis.

In this work, we applied GSIT to synthesize 2D silver nanocrystals.[†] The interaction of gaseous N_2H_4 with the surface of the silver salt solution for 1 h provided a thin film on the solution surface. The SEM images [Figure 1(*a*),(*b*)] show that the film consists of flat particles 10–60 nm thick and more than 10 μm^2 surface area. Most of Ag particles were crystallized in hexagonal

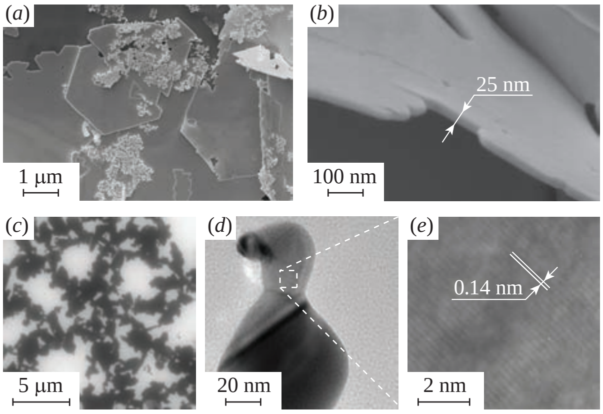

Figure 1 Electron microscopy images of the Ag 2D nanocrystals synthesized at the surface of a 0.01 M AgOAc solution by GSIT: (*a*) overview SEM image, (*b*) cross-sectional view SEM images, (*c*) overview TEM image, (*d*) TEM image of a single particle and (*e*) HRTEM of a selected particle area.

[†] AgOAc (chemically pure from ZAO Dinz), NH_4OAc (pure from Vecton) salts and hydrazine hydrate $(NH_2)_2\cdot H_2O$ (from Lenreactiv) were used as reactants. Aqueous solutions were prepared using Milli-Q high purity water with a resistivity higher than 18 MΩ cm^{-1}. To study the formation of particles at the interface, the ratio between NH_4OAc and AgOAc concentrations in solution was varied from 1 to 25. The NH_4OAc salt provided the state of silver forms in solution and a suitable value of pH 6.2, and it acted as a capping reagent. We used a 0.01 M AgOAc and 0.125 M NH_4OAc mixed solution as an optimal reagent for the reproducible crystal growth of silver nanoplates. The silver salt solution was poured into a flat Teflon vessel located in a hermetically sealed Teflon lined chemical reactor and treated by gaseous N_2H_4 for 5–60 min at room temperature. The particles formed on the solution surface were transferred carefully onto the surface of distilled water and left for 10 min to remove an excess of the reagent solution. The procedure was repeated twice, and the film was transferred to the silicon–wafer surface and dried at room temperature. The support was washed in acetone to remove organic impurities and etched for 10 min in a 'piranha' solution (a mixture of H_2O_2 and concentrated H_2SO_4 in a volume ratio of 3 : 7) with simultaneous ultrasonic cleaning (60 W) to prepare a hydrophilic surface and then rinsed thoroughly in water.

The prepared samples on silicon surfaces were studied by scanning electron microscopy (SEM), XRD analysis and optical microscopy. The morphology was studied using Zeiss EVO-40EP or Supra VP-40 Zeiss Merlin instruments. X-ray powder diffraction analysis was performed on a Bruker D2 Phaser diffractometer equipped with a CuKα X-ray source. The TEM and HRTEM images were taken on a Zeiss Libra 200 FE transmission electron microscope after transferring the as-synthesized particles from water surface onto an Au grid coated with a carbon support film.

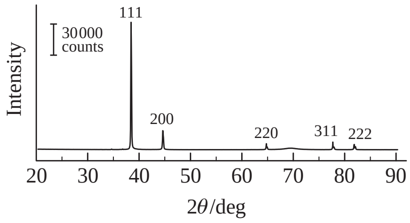

Figure 2 X-ray diffraction pattern of the synthesized silver crystals transferred onto a silicon surface, λ = 1.5406 Å.

shape nanoplates. The internal angle of a typical crystal was 120°. A number of large particles exhibited unusual jagged borders with triangular cutouts.

The TEM overview image [Figure 1(*c*)] of the sample prepared by GSIT for 20 min shows that the formation of a continuous film was not completed. In this time, the Ag nanoplates have a surface area of 3 μm^2 and their aggregate forms a fractal-like network. Figures 1(*d*),(*e*) demonstrate a particle with typical defects, which originate in crystal growth process, and HRTEM image of a selected area of single Ag particle with clear crystal lattice.

Figure 2 shows X-ray diffraction patterns for Ag particles obtained by GSIT and transferred onto a silicon surface. A series of diffraction peaks was assigned to the crystal planes of silver with space group *Fm*-3*m*.[35] No further peaks corresponding to other compounds were observed. The diffraction pattern is dominated by the (111) peak of silver, indicative of this crystal faces parallel to the support.

Let us consider a model of the crystal growth of silver 2D nanocrystals under interfacial reaction conditions. According to hydrochemical equilibrium calculations by the Hydra–Medusa program,[36] the silver ions can be stabilized as AgOAc species in a reagent solution with suitable concentration and pH. Another part of the system is hydrazine, which can serve as a reducing agent from a gaseous phase. At the initial time of interaction, Ag seeds are formed on the surface of liquid reagent and surface tension of water solution keeps them on surface. Acetate ions adsorbed onto the (111) surface of Ag crystals predominantly[37] acted as a capping agent. After that, anisotropic crystal growth can be detected in the direction (110). At the next stage of interaction, nanoplates coat the main part of solution surface and the oriented attachment growth can became a dominant way to form giant 2D particles with large surface areas. In our case, we observed typical crystal defects in silver 2D particles, namely, twin planes in crystals and specific jagged borders. In accordance with published data,[38,39] these characteristic structural defects indicate the presence of oriented attachment growth between the edge surfaces of adjacent nanoplates. As found earlier,[21] the nanoplates of silver are thermodynamically unstable due to their high surface energies resulting from their large surface area. Therefore, the presence of structural defects in 2D crystals growing at a gas–solution interface is predictable. Figure 3 illustrates a possible model of silver 2D particle fabrication.

In our opinion, the proposed synthesis of 2D silver crystals is characterized by the following advantages over the traditional ways. The fast and facile synthesis is carried out at room temperature with a simple experimental installation, and the typical processing time is no longer than 1 h. The stage of particle separation from the solution by multiple washing and repeated centrifugation is not required. The produced silver 2D particles are free from organic surfactants or capping agents as a result of the templateless and surfactant-free synthesis. The formation of a uniform film or network structure can be achieved by simple transfer onto a flat substrate.

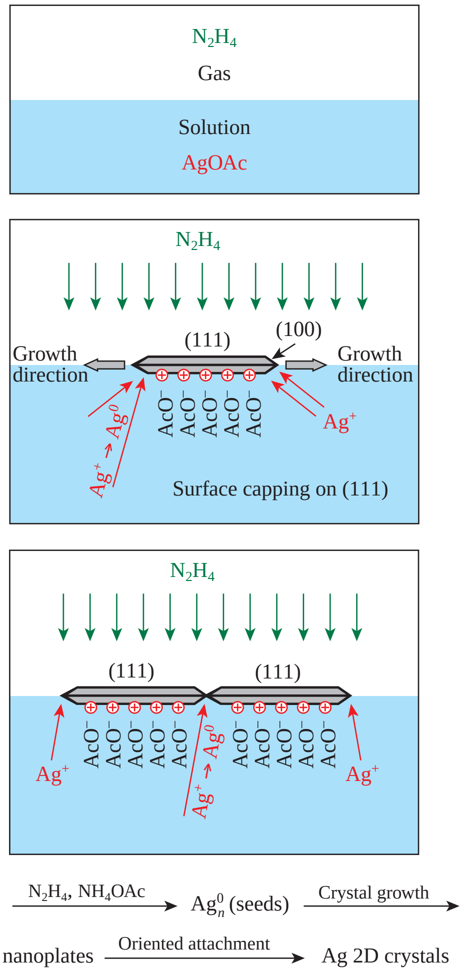

Figure 3 Model of the crystal growth of silver 2D nanocrystals by GSIT.

In conclusion, the 2D silver crystals can be synthesized at the gas–solution interface by the interaction of a mixed aqueous solution of AgOAc and NH_4OAc salts with gaseous N_2H_4. The thickness of the 2D nanocrystals is about 10–60 nm and the surface area is more than 10 μm^2. The crystal structure of 2D nanocrystals is a face-centered cubic lattice with crystal defects originated from the oriented attachment mechanism of crystal growth.

We expect that nanosized material based on 2D silver crystals is promising for all applications typical of conducting 2D nanomaterials.

This study was supported by the Russian Foundation for Basic Research (grant no. 15-03-08045). The XRD analysis was carried out at the X-ray Diffraction Centre of St. Petersburg State University. The SEM, TEM and HRTEM studies were performed at the Nanotechnology Centre of St. Petersburg State University.

References

1 B. Wiley, Y. Sun, B. Mayers and Y. Xia, *Chem. Eur. J.*, 2005, **11**, 454.
2 X. Li, L. Wang and G. Yan, *Cryst. Res. Technol.*, 2011, **46**, 427.
3 T. Sannicolo, M. Lagrange, A. Cabos, C. Celle, J. P. Simonato and D. Bellet, *Small*, 2016, **12**, 6052.
4 A. Morag and R. Jelinek, *J. Colloid Interface Sci.*, 2016, **482**, 267.
5 X. Lu, M. Rycenga, S. E. Skrabalak, B. Wiley and Y. Xia, *Annu. Rev. Phys. Chem.*, 2009, **60**, 167.
6 M. O. Volodina, A. Yu. Polyakov, A. V. Sidorov, A. V. Grigorieva, E. A. Eremina, S. V. Savilov and E. A. Goodilin, *Mendeleev Commun.*, 2016, **26**, 231.
7 A. A. Semenova, N. A. Braze, G. V. Maksimov, I. A. Semenova, A. P. Semenov and E. A. Goodilin, *Mendeleev Commun.*, 2016, **26**, 32.

8 S. Dagostino and F. Della Sala, *J. Phys. Chem. C*, 2011, **115**, 11934.
9 M. Yan, Y. Xiang, L. Liu, L. Chai, X. Li and T. Feng, *RSC Adv.*, 2014, **4**, 98.
10 H. Zheng, D. Ni, Z. Yu, P. Liang and H. Chen, *Sens. Actuators, B*, 2016, **231**, 423.
11 G. Korotcenkov, B. K. Cho, L. B. Gulina and V. P. Tolstoy, *Sens. Actuators, B*, 2012, **166–167**, 402.
12 G. Korotcenkov, B. K. Cho, L. B. Gulina and V. P. Tolstoy, *World Acad. Sci. Eng. Technol.*, 2011, **81**, 199.
13 L. B. Gulina, G. Korotcenkov, B. K. Cho, S. H. Han and V. P. Tolstoy, *J. Mater. Sci.*, 2011, **46**, 4555.
14 E. V. Dokuchits, A. V. Khasin and A. A. Khassin, *Mendeleev Commun.*, 2015, **25**, 155.
15 B. S. Bal’zhinimaev, V. I. Zaikovskii, L. G. Pinaeva, A. V. Romanenko and G. V. Ivanov, *Mendeleev Commun.*, 1998, 100.
16 N. G. Bastús, F. Merkoçi, J. Piella and V. Puntes, *Chem. Mater.*, 2014, **26**, 2836.
17 M. H. Rashid and T. K. Mandal, *J. Phys. Chem. C*, 2007, **111**, 16750.
18 Z. Huang, X. Jiang, D. Guo and N. Gu, *J. Nanosci. Nanotechnol.*, 2011, **11**, 9395.
19 A. A. Semenova, A. P. Semenov, E. A. Gudilina, G. T. Sinyukova, N. A. Brazhe, G. V. Maksimov and E. A. Goodilin, *Mendeleev Commun.*, 2016, **26**, 177.
20 N. B. Golovina and L. M. Kustov, *Mendeleev Commun.*, 2013, **23**, 59.
21 Z. Liu, H. Zhou, Y. S. Lim, J.-H. Song, L. Piao and S.-H. Kim, *Langmuir*, 2012, **28**, 9244.
22 K. Aslan, J. R. Lakowicz and C. D. Geddes, *J. Phys. Chem. B*, 2005, **109**, 6247.
23 H.-M. Ren, Y. Guo, S.-Y. Huang, K. Zhang, M. M. F. Yuen, X.-Z. Fu, S. Yu, R. Sun and C.-P. Wong, *ACS Appl. Mater. Interfaces*, 2015, **7**, 13685.
24 X. Zhao, B. Chen, C. Li, T. Wang, J. Zhang, X. Jiao and D. Chen, *Chem. Eng. J.*, 2016, **285**, 690.
25 C.-W. Chang, F.-C. Lin, C.-Y. Chiu, C.-Y. Su, J.-S. Huang, T.-P. Perng and T.-J. Yen, *ACS Appl. Mater. Interfaces*, 2014, **6**, 11791.
26 C.-Y. Wang, H.-Y. Chen, L. Sun, W.-L. Chen, Y.-M. Chang, H. Ahn, X. Li and S. Gwo, *Nat. Commun.*, 2015, **6**, 7734.
27 P. Jia, J. Chang, J. Wang, P. Zhang, B. Cao, Y. Geng, X. Wang and K. Pan, *Chem. Asian J.*, 2016, **11**, 86.
28 G. Wu, S. Yang and Q. Liu, *Appl. Surf. Sci.*, 2015, **357**, Part A, 583.
29 V. P. Tolstoy and L. B. Gulina, *J. Nano-Electron. Phys.*, 2013, **5**, 01003.
30 V. P. Tolstoy and L. B. Gulina, *Langmuir*, 2014, **30**, 8366.
31 L. B. Gulina, V. P. Tolstoy, I. A. Kasatkin and Y. V. Petrov, *J. Fluorine Chem.*, 2015, **180**, 117.
32 L. B. Gulina, M. Schäfer, A. F. Privalov, V. P. Tolstoy and I. V. Murin, *J. Chem. Phys.*, 2015, **143**, 234702.
33 L. B. Gulina, M. Schäfer, A. F. Privalov, V. P. Tolstoy, I. V. Murin and M. Vogel, *J. Fluorine Chem.*, 2016, **188**, 185.
34 L. B. Gulina, V. P. Tolstoy, A. A. Lobinsky and Yu. V. Petrov, *Russ. J. Gen. Chem.*, 2016, **86**, 2689 (*Zh. Obshch. Khim*., 2016, **86**, 2057).
35 I.-K. Suh, H. Ohta and Y. Waseda, *J. Mater. Sci.*, 1988, **23**, 757.
36 I. Puigdomenech, *HYDRA (Hydrochemical Equilibrium-Constant Database) and MEDUSA (Make Equilibrium Diagrams Using Sophisticated Algorithms) Programs*, www.kemi.kth.se/medusa.
37 Q. Zhang, N. Li, J. Goebl, Z. Lu and Y. Yin, *J. Am. Chem. Soc.*, 2011, **133**, 18931.
38 V. K. Ivanov, P. P. Fedorov, A. Y. Baranchikov and V. V. Osiko, *Russ. Chem. Rev.*, 2014, **83**, 1204.
39 W. Lv, W. He, X. Wang, Y. Niu, H. Cao, J. H. Dickerson and Z. Wang, *Nanoscale*, 2014, **6**, 2531.

Received: 13th February 2017; Com. 17/5177